Pulse Duration Dependent Mid-Infrared Laser Ablation for Biological Applications

Mark A. Mackanos, Dmitrii M. Simanovskii, Kenneth E. Schriver, M. Shane Hutson, Christopher H. Contag, John A. Kozub, and E. Duco Jansen

(Invited Paper)

***Abstract*— There are significant benefits to medical laser surgeries performed with mid-infrared wavelengths, including the ability to select laser parameters in order to minimize photochemical and thermal collateral damage. It has been shown that a wavelength of 6.1 micrometers (μm) is optimal when high ablation efficiency and minimal collateral damage is desired in biological soft tissues. Historically, free electron lasers were the only option for ablating tissue at this wavelength due to their ample pulse energy and average power. In recent years new sources are being developed for this wavelength that can successfully ablate tissue. These alternative sources have different pulse structures and pulse durations than free electron lasers, motivating investigation of how these parameters affect the ablation process. Here, we present the pulse duration dependence for mid-IR laser ablation of biological tissues at a wavelength of 6.1 μm on a tissue phantom of cooked egg white. The crater shape, depth, and volume all changed in a significant, non-monotonic manner as the laser pulse duration was increased from 100 ns to 5 μs.**

***Index Terms*— Mid-infrared laser ablation, pulse duration, Pockels cell, tissue ablation, crater shape, crater depth, crater volume, Free Electron Laser (FEL), Optical Parametric Oscillator (OPO).**

Manuscript received September 16, 2011. This work was supported by the U. S. Air Force Office of Scientific Research, Grant No. F49620-00-1-0349.

M. A. Mackanos is with the Departments of Pediatrics, Microbiology and Immunology, and Radiology: Molecular Imaging Program at Stanford (MIPS) and the BioX Program, Stanford University, Stanford, CA 94305 and the W.M. Keck Vanderbilt Free Electron Laser Center and the Department of Biomedical Engineering, Vanderbilt University, Nashville, TN 37235 (e-mail: mark.mackanos@vanderbilt.edu).

D. M. Simanovskii is with the Hansen Experimental Physics Laboratory, Stanford University, Stanford, CA 94305 (e-mail: simanovskii@gmail.com).

K. E. Schriver is with the Department of Physics and Astronomy, Vanderbilt University, Nashville, TN 37235 (e-mail: ken.schriver@vanderbilt.edu).

M. Shane Hutson is with the W. M. Keck Vanderbilt Free Electron Laser Center and the Department of Physics and Astronomy, Vanderbilt University, Nashville, TN 37235 (e-mail: shane.hutson@vanderbilt.edu).

C. H. Contag is with the Department of Pediatrics, Microbiology and Immunology, and Radiology: Molecular Imaging Program at Stanford (MIPS) and the BioX Program, Stanford University, Stanford, CA 94305 (e-mail: ccontag@stanford.edu).

J. A. Kozub is with the W. M. Keck Vanderbilt Free Electron Laser Center, Vanderbilt University, Nashville, TN 37235 (e-mail: john.kozub@vanderbilt.edu).

E. D. Jansen is with the W. M. Keck Vanderbilt Free Electron Laser Center and the Department of Biomedical Engineering, Vanderbilt University, Nashville, TN 37235 (phone: 615-343-1911, fax: 615-343-7919, e-mail: duco.jansen@vanderbilt.edu).

I. INTRODUCTION

There are many properties of biological tissues that affect pulsed laser ablation. Tissue optical properties determine the internal energy distribution that initiates the ablation process[1]. The structure and morphology of tissue also affects energy transport within its constituents[2] and, along with mechanical and thermal properties, controls the response of tissue to pulsed heating and phase transformation[1]. Strong absorption of energy in tissues occurs in both the ultraviolet and mid-infrared wavelength regions; however, due to the potential mutagenic effects of ultraviolet wavelengths, mid-infrared laser radiation is preferred for many types of tissue, in particular in tissues with high cellularity[3]. The wavelengths of greatest interest for mid-infrared pulsed laser ablation have traditionally been at 2.1, 2.94, 6.1, 6.45, and 10.6 μm due to either the ability to remove tissue with little concomitant thermal damage or the availability of laser sources at these wavelengths[1, 3-14]. The absorption of mid-IR radiation at 2.1, 2.94, and 10.6 μm is primarily associated with strong water absorption; however, water and protein both absorb at 6.1 and 6.45 μm which coincide with the amide-I and amide-II absorption bands of protein respectively[1]. The promising results first obtained at the Vanderbilt University Mark-III free electron laser (FEL) were initially attributed to the absorbance of the protein in addition to the water in the tissue[4]. The absorption of collagen is twice that of water at 6.1 μm and six times that of water at 6.45 μm. In addition, the water absorption at 6.1 μm is 3.5 times higher than it is at 6.45 μm. Recent work has shown that 6.1 μm wavelength light gives improved tissue ablation with minimal thermal damage for numerous tissue types[9, 14-21]. To date, the Vanderbilt FEL has been used for a total of eight human surgeries including neurosurgery and ophthalmic surgery[6, 22-27]; however, the prohibitive size and cost of an FEL limits its practicality for medical uses. Although the wavelength range described here allows for selective excitation of amide bands, the lifetimes of these vibrations are only in the picosecond range[28-31]. Recently, researchers have shown that mid-IR laser ablation in the picosecond pulse duration range may have benefits in efficient ablation related to vibrational excitation to both hard and soft tissues[32, 33]; however, on the time scale of the FEL pulsewidth (100 ns to 5 μs), selective excitation is relatively unimportant and thermal processes dominate.

Alternative laser sources in the 6-8 μm range are currently being developed and tested for numerous medical applications, including an Er:YSGG pumped $ZnGeP_2$ crystal optical parametric oscillator (OPO)[9, 34], an Er:YAG pumped $AgGaSe_2$ OPO[35, 36], and a Raman-shifted Alexandrite laser[37]. Recently quantum cascade lasers have been shown to provide numerous wavelengths in the region of interest; however, these lasers are currently limited to spectroscopy applications due to their cw operation and energy limitations[38-40]. In addition to wavelength, a critical parameter that needs to be specified in the development of these laser sources is the pulse duration. We have previously shown that the micropulse structure of the FEL (each 5 μs macropulse consists of ~14,000 micropulses approximately 1 picosecond in duration delivered at 2.85 GHz) plays a negligible role in the ablation characteristics of the FEL[7, 8]; however, the role of the macropulse duration in achieving efficient tissue ablation and minimal collateral damage has not been well defined. Therefore, it was our goal with this research to explore the pulse duration dependence for 6.1 μm laser ablation of biological tissues.

The pulse duration of the ZGP:OPO system (λ=6.1 μm) used in previous work was 100 ns[9]. When compared to ablation using the FEL, significant differences were found in the ablation rate as well as in the size and shape of the ablation craters produced in cornea. The ZGP:OPO showed a significantly higher ablation rate with all other parameters being held constant except for the repetition rate. To determine the effect of pulse duration on crater size, shape, and ablation efficiency, we needed to vary the pulse duration over the range from the 5 μs native FEL macropulse to the 100 ns width of the ZGP:OPO. Given the large macropulse energy available with the FEL, it is possible to shorten the FEL macropulse to as little as 100ns and still have enough energy to ablate tissue with a single pulse. By using a Pockels cell, we were able to slice a portion of the FEL macropulse and thus produce pulses with variable durations from the maximum 5 μs to as short as 100 ns over a range of pulse energies[41, 42].

Previous research using gelatin as a tissue phantom yielded only limited results for analysis due to melting and re-coagulation of the gelatin following ablation; even when measurements were performed on craters made in gelatin with a single laser pulse, accurate results were not always obtained. Therefore, we decided to use cooked egg white as our tissue phantom since its water/protein constituency mimics that of biological soft tissue and it does not melt and re-coagulate during or following laser ablation.

II. Mid-Infrared Laser Ablation

A. Laser System

The laser system used for ablation was the Vanderbilt Mark III Free Electron Laser (FEL)[4, 43-45]. The laser was operated with a 30 Hz pulse repetition frequency, a 2.856 GHz micropulse repetition frequency, and an emission wavelength centered at 6.1 μm. The laser beam was sent through a 6 mm diameter, λ=4-8 μm Pockels cell (II-VI Inc., Saxonburg, PA), operated with a high voltage Behlke switch triggered by a TTL pulse synchronized with the FEL pulse train and an electrical one-shot box operating a fast shutter to select single macropulses. A digital delay generator (Stanford Research Systems, DG535) was used to trigger the Pockels cell and shorten the 5 μs FEL laser macropulse to the pulse durations of interest down to 100 ns. After confirming that the spatial beam profile resembled a Gaussian, the laser beam radius was analyzed using a knife-edge measurement[46] in front of a pyroelectric detector (J-25, Molectron Inc.), and determined to be ~47 μm (+/- 5% due to detector uncertainty) for all of the experiments performed.

B. Ablation Threshold Measurements

The laser ablation threshold was measured on both water and cooked egg white using a red HeNe laser beam directed tangentially across the target surface at the FEL laser ablation location. The red HeNe beam reflected from ablated water and/or egg white passed through an optical iris to a CCD detector. The CCD detector signal was then sent to an oscilloscope for analysis. The laser pulse energy was adjusted until the signal due to reflected light from the ablated sample was seen; this gave an accurate reading for the ablation threshold at all pulse durations investigated between 5 μs and 100 ns.

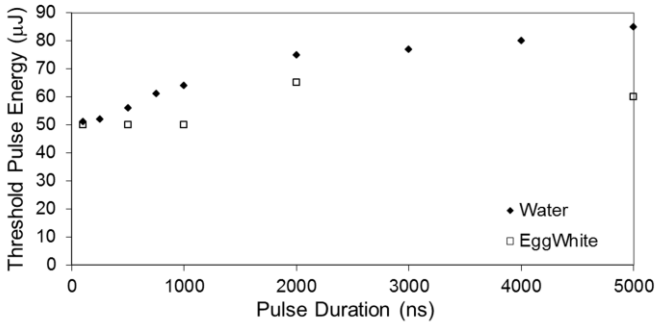

Fig. 1. The ablation threshold in μJ versus pulse duration in nanoseconds for all of the durations of interest in water and the key pulse durations in cooked egg white for comparison with a 47 μm radius spot size.

We first determined the threshold of ablation for both water and cooked egg white at the different 6.1 μm pulse durations. Due to the loss of energy with shorter pulses out of the Pockels cell, we decided to use as small a spotsize as was practical (~47 μm radius). Nine pulse durations were used between 100 ns and 5 μs as shown in figure 1. For cooked egg white irradiated with pulses at 6.1 μm in wavelength, the threshold energy for ablation was determined to be 50 +/- 10 μJ at the spot size used, giving a threshold radiant exposure of approximately 0.72 J/cm^2. There was no significant change in the threshold for the ablation of egg white over the range of pulse durations used as seen in figure 1.

III. Pulse Duration dependence of crater Formation, Depth, and Shape

A. Crater Formation

A single pulse at 6.1 μm was used to ablate a fresh piece of cooked egg white that was placed on a translation

stage and kept at room temperature (21 ^{o}C). A micrometer was used to move the translation stage a distance of 1 mm between subsequent laser pulses. The energy was changed between 75 and 225 μJ using a ZnSe polarizer/attenuator (II-VI Inc.). The pulse energy was measured using a J-25 detector (Molectron Inc.).

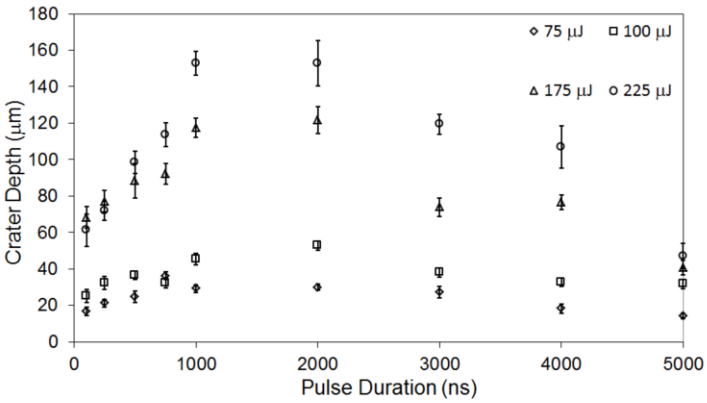

Fig. 2. The single pulse induced crater depth in μm produced as a function of pulse duration (ns) at 75, 100, 175, and 225 μJ of energy per pulse. A minimum of 10 craters were averaged for each point. The error bars are the standard deviation for the ten craters. The deepest craters were found at 1,000 and 2,000 ns in pulse duration.

B. Crater Depth Measurements

The crater depth was measured and averaged for a minimum of 10 craters at each pulse duration and pulse energy with an Olympus Fluoview laser scanning confocal microscope with FV300 software and an Olympus BX-VCB motion controller which allowed for depth measurement with a precision of 10 nm. Given the 100 mJ of energy available in a 5 μs pulse from the FEL, we were able to compare single pulse ablation craters for all pulse durations over a wide range of pulse energies all well above the ablation threshold energy (75, 100, 175, and 225 μJ). Comparison of craters made with equal pulse energies but widely different pulse widths revealed substantial differences in their shape, and prompted a detailed characterization of the pulse duration-dependence of ablation craters produced with these laser parameters. The results (figure 2) show that the deepest craters were made at 1,000 and 2,000 ns in pulse duration. The shallowest craters were produced with pulse durations of 100 ns and 5,000 ns.

C. Crater Shape Measurements

While crater depth is a common parameter for determining the overall ablation rate, the shape of the crater must also be measured in order to determine the volume of material removed (and hence get a handle on the overall ablation efficiency). The crater shape was measured using the same laser scanning microscope as described above. The

diameter of the crater was measured beginning at the surface of the egg white and then measured repeatedly at deeper and deeper locations in the crater until the bottom of the crater was seen. This was repeated for a minimum of three craters at each pulse duration. All crater shapes were analyzed at a constant pulse energy of roughly 3 times the ablation threshold (175 μJ) for reproducibility.

The average diameter was then plotted as a function of depth to construct a cross section through the crater. The resulting crater shapes revealed a pulse duration dependence shown in figure 3. The deepest craters are again seen at 1,000 and 2,000 ns; however, there was a marked change in the shape of the craters through this range of pulse durations. The craters get wider as the pulse duration gets shorter, with the widest crater being seen at 100 ns. This crater was more than twice the diameter of the Gaussian beam diameter that was used to create it. In addition, the widest short pulse crater is almost hemispherical, quite unlike the narrow, conical-shaped crater produced by the longest (5,000 ns) pulse.

D. Crater Volume Measurements

Each crater shape is approximated by a curve specifying the radius as a function of the crater depth. We calculated volumes by integrating over the crater depth using a polynomial function to fit the radial profile that was determined in the crater shape analysis as described above. The integration was performed using Microcal Origin 6.0 software. The total volume of the single pulse craters was calculated from the data and plotted as a function of pulse duration; these results are shown in figure 4. For each pulse energy, the volume of tissue removed *increases* with a decreasing pulse duration. The largest volume of tissue was removed with the 100 ns pulse and the smallest volume was removed with the 5,000 ns pulse duration. A sharp decrease in crater volume occurred near 1,000 ns, which corresponds to the shape change seen in figure 3; this may coincide with the onset of steady-state tissue ejection and plume screening[10].

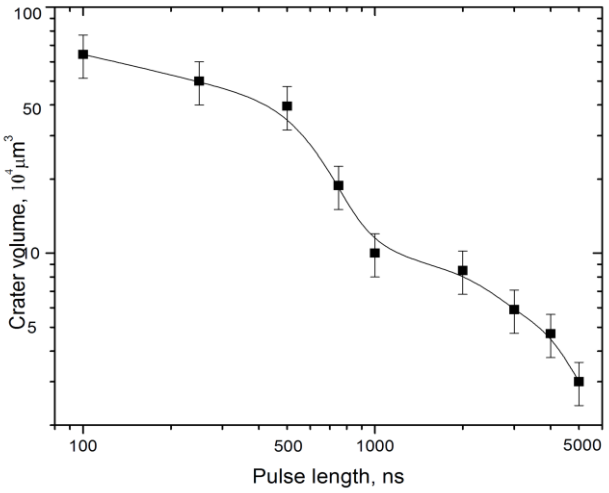

Fig. 4. The crater volume for each of the nine pulse durations is shown in 10^4 μm^3 versus pulse duration in nanoseconds. The error bars are the standard deviation for the average of at least three craters for each pulse duration.

E. Mathematical Modeling

Multiple physical mechanisms could impact the pulsewidth-dependence of crater depth and shape. To better understand these interacting mechanisms, we constructed a phenomenological model based on time-delay partial differential equations. This model includes a transition from blow-off type behavior – i.e. material removal occurs only after the pulse – to a process of continuous material removal during the pulse and its associated plume screening.

The model is simplified because the role of thermal diffusion is minimal. Egg white is largely denatured protein and should have a thermal diffusivity similar to that of protein, $\alpha = 8.1 \times 10^{-8}$ m^2/s [47]. Even for the longest pulses used here, the characteristic thermal diffusion distance is just $(\alpha\tau)^{1/2} \sim 0.6$ μm, much smaller than any of the observed crater dimensions. Thermal diffusion would not become important until the pulsewidths approached the characteristic thermal diffusion times: $\tau_{Radial} \sim w^2/\alpha \sim 2.7$ ms based on a $1/e^2$ beam radius of 47 μm; and $\tau_{Axial} \sim \delta^2/\alpha \sim 170$ μs based on an absorption depth of 3.7 μm. Given these estimates, our model excludes thermal diffusion.

Existing mathematical models can reproduce the range of observed crater shapes, but fail to account for the pulsewidth-dependence, and do not reproduce the correct coupling of crater shape and depth. For short pulsewidths (100-500 ns), we observe rounded craters that are in reasonable agreement with a blow-off model [48]:

$$z(r) = d \ln\left[\frac{F(r)}{dH_{abl}}\right]$$

where $z(r)$ is the crater depth at distance r from the beam axis, $F(r)$ is the fluence δ is the absorption depth and H_{abl} is the threshold energy density for material removal. To match the observed crater depths, one must assume an extremely low H_{abl} ($< 10^{-4}$ J/cm^3) and/or dynamic optical properties that yield a dramatic increase in the absorption depth. To match the observed trends in crater depth, one would need to assume a pulsewidth-dependence for one or both parameters. For longer pulsewidths, we observe craters that transition from Gaussian to sharply peaked trumpet shapes. These shapes can all be reproduced by "steady-state" models that assume continuous material removal at a rate that is proportional to the projection of the intensity normal to the current crater surface [49, 50]:

$$\frac{\partial z(r,t)}{\partial t} = \frac{F(r)}{t H_{abl}}\left[1 + \left(\frac{\partial z(r,t)}{\partial r}\right)^2\right]^{\frac{1}{2}}$$

These models assume the absorption depth is small compared to the size of the crater, neglect surface reflection, and neglect any absorption or scattering in the ejected material. Nonetheless, the models yield Gaussian-shaped craters at near-threshold fluence and sharply peaked trumpet-shaped craters at higher fluence. One can get a similar range of crater shapes by recasting this model as a condition on the slope of the final crater wall[51]. For a given fluence, both versions of the model predict identical crater shapes regardless of pulsewidth. This becomes clear if one casts the model in integral form and switches the integration variable to t/τ:

$$z(r,t) = \int_0^t \frac{F(r)}{H_{abl}} \left[1 + \left(\frac{\partial z(r,t')}{\partial r}\right)^2\right]^{\frac{1}{2}} dt'$$

The model thus cannot reproduce the observed transition in crater shape at constant fluence, but variable pulsewidth. Furthermore, the steady-state models yield results in which deeper craters are always sharper – in contradiction with the experimental results.

To better match our experimental results, we thus constructed a hybrid of the blow-off and steady-state models. We chose the most straightforward combination by assuming that there is a shortest time, τ_{eject}, at which material removal begins. At $t = \tau_{\text{eject}}$, material is removed according to a blow-off model. After this time, material is removed continuously at a rate that depends on the projection of the intensity normal to the crater surface and screening by previously ablated material. Mathematically, the model can be expressed as:

$$z(r, t_{eject}) = d \ln\left[\frac{F(r)}{dH_{abl,BO}} \frac{t_{eject}}{t}\right]$$

$$\frac{\partial z(r, t > t_{eject})}{\partial t} = \frac{F(r)}{t H_{abl,SS}} \left[1 + \left(\frac{\partial z(r, t - \Delta_1)}{\partial r}\right)^2\right]^{\frac{1}{2}} S(r, t - \Delta_2)$$

where $S(r,t-\Delta_2)$ is a function that accounts for plume screening, and Δ_1 and Δ_2 are delays that respectively account for the time required to form a well-defined crater interface and a highly attenuating plume of ejected material. We investigated several screening functions and found that the best results were obtained by integrating all of the material removed and distributing this material in an annular plume – similar to that observed upon impact ejection from a fluid surface[52]. The mathematical form for this screening function is:

$$S(r, t - \Delta_2) = e^{-\left(P(r)\int_0^t \int_0^\infty z(r,t'-\Delta_2) 2\pi r\, dr\, dt'\right)/d_{plume}}$$

where δ_{plume} is the absorption depth of the plume and the integrals calculate the total amount of material in the plume up to time $t-\Delta_2$. The normalized function $P(r)$ contains all information about the annular shape of the plume and was assumed to be a Gaussian of width w centered at $r = w$.

These partial differential equations were cast as coupled time-delay ordinary differential equations with radial derivatives approximated by finite differences. The equations were then numerically integrated in Mathematica (Wolfram, Champaign, IL). Integration of the ejected material in the plume was performed out to a radial distance of 5w.

Figure 5 shows model solutions for a particular set of global parameters (details in figure caption). These parameters were chosen to match the trends in crater shape and depth observed in experiments. The crater shapes transition from rounded to Gaussian to sharply peaked and the crater depth first increases with pulsewidth and then decreases, with a maximum crater depth of 120 μm reached at $\tau = 1000$ ns.

If one varies each temporal parameter from its selected value, one observes characteristic changes in the crater shapes and depths. τ_{eject} and Δ_1 determine the pulsewidth scale on which the crater shape transitions from rounded to Gaussian. Δ_1 and Δ_2 then determine the pulsewidth scale on which the craters become sharply peaked. For the longest

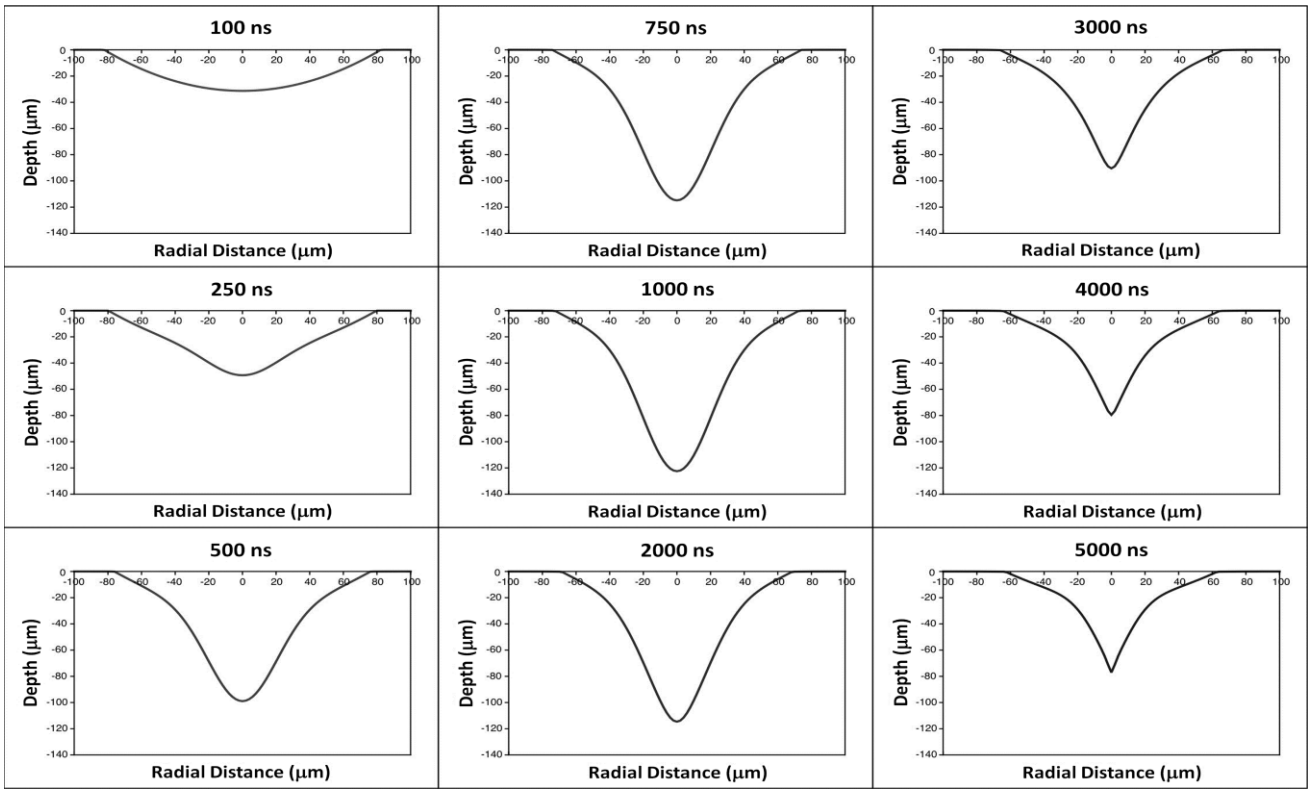

Fig. 5. Calculated crater shapes for pulsewidths between 100 and 5000 ns. All calculations used the same global parameters: $E_{\text{pulse}} = 175$ μJ, $w = 47$ μm, $H_{abl,BO} = 4$ J/cm^3, $H_{abl\_SS} = 400$ J/cm^3, $\tau_{\text{eject}} = 150$ ns, $\Delta_1 = 800$ ns, $\Delta_2 = 1600$ ns, and $\delta = \delta_{plume} = 3.7$ μm. The plume shape was assumed to be annular with a Gaussian density centered at $r = w$ with a $1/e^2$ width w.

pulses, both the slope factor and the plume screening function are necessary to generate sharply peaked craters even as the crater depth decreases. If one excludes plume screening in the model (e.g. by letting δ_{plume} go to ∞), the craters for $\tau > 2000$ ns still become sharply peaked, but they all have the same depth. If one includes plume screening with a uniform plume, the long pulse craters become shallower, but also more rounded. Only screening with an annular plume matches the trends in both the crater shape and depth.

The model presented here is phenomenological. More fundamental modeling would require an explicit consideration of the kinetics of explosive vaporization in a mechanically constrained tissue, the time-dependent shape of the ejected plume and the impact of this plume on how incoming radiation reaches the underlying tissue. The equilibrium properties of water and steam are very well known; however, the kinetics of the phase transition are not as well understood, particularly under the extreme conditions of laser ablation. These are active areas of research and future results should improve the ability to model the relevant hydrodynamics.

IV. Observations and Benefits for Future Laser Development

The observed transition from a wide, nearly hemispherical crater shape to a narrow, conical shape suggests that two different mechanisms for ablation are involved over this range of pulse durations. The short pulses deliver the entire pulse energy (3 times the ablation threshold) to a small volume of tissue before significant heat diffusion can take place; this results in an explosive phase change, which would leave a hemispherical crater. This mechanism acts like a 'blow off' model which would remove a larger volume of material[53]. With the longer pulses, a slower mechanism such as an equilibrium state of evaporative boiling may occur ('steady state' model)[53]. In this case, tissue would be removed in a continuous fashion as long as energy required for boiling is being deposited in tissue faster than it is being lost through diffusion and plume screening. This argument is supported by the proximity of the thermal diffusion time to the 5 μs pulse width at the 6.1 μm wavelength[54]. Since the laser intensity is weaker around the edges of the beam, longer pulse durations limit ablation to the central portion of the irradiated spot, where losses from heat diffusion and plume screening could still be overcome. Therefore, a small, narrow crater would be produced. The abrupt change in crater shape seen at pulse durations around 1,000 ns is consistent with the onset of large amounts of material being removed (and strong plume screening). The shrinking crater size observed with pulses longer than ~1,000 ns can be explained by the loss of incident laser radiant exposure to plume screening. Previous work showed the development of a water plume prior to the end of the 5000 ns pulse during ablation of water using the FEL that causes plume screening during the long FEL pulse duration[7].

While the largest volume of material was removed with the shortest pulses, the deepest craters resulted from the intermediate pulse durations. We propose the following explanation: with the shortest pulses, tissue may reach radiant exposures well in excess of the threshold needed for ablation; the extra energy would be lost to pressure waves in the bulk of the tissue or to kinetic energy of material in the plume. With longer pulses, there is more time for energy transfer into deeper regions of the tissue, so that more of the available laser energy could be used to remove tissue from underneath the center of the irradiated area. This could result in the deeper (but narrower) craters found with intermediate laser pulse durations. In addition, thermal lensing becomes more of a pronounced interaction in tissue with longer pulse durations. As a result, the laser beam divergence may increase which will reduce the area of the tissue that reaches the ablation threshold [55-57]. These factors could lead to a deeper and narrower crater shape for the intermediate pulse durations as compared to the short pulse durations.

V. Conclusion

Using the Vanderbilt Mark III free electron laser (FEL) and cooked egg white as our tissue phantom allowed us to perform a thorough study of the laser pulse duration dependence of ablation at 6.1 μm in wavelength. We were able to compare nine different pulse durations from 5,000 ns down to 100 ns. The 100 ns pulse duration is comparable with the pulse durations typically used in alternative laser sources, such as the ZGP:OPO laser system, in this mid-infrared wavelength range. This work did not cover the ~10 ns range, where several new mid-IR generation schemes are being developed. Our results suggest that such short pulses might result in even larger total volumes and shallower craters. We were able to vary single pulse energies from just above the threshold for ablation to four and a half times the threshold, and performed a detailed comparison of crater depth, crater shape, and crater volume at a fixed pulse energy three and a half times the ablation threshold. We found that the deepest craters were achieved at 1,000 ns while the largest crater volume was removed with 100 ns pulses, suggesting that a short pulse at 6.1 μm is preferred for removing large surface areas of tissue, while a longer pulse is preferred for a deep and narrow cut. Mathematical modeling with a hybrid of blow-off and steady-state models and the inclusion of plume screening is able to reproduce the observed trends in both crater shape and depth. The results obtained in this work provide a great potential for understanding tissue removal in laser medical applications in the mid-infrared region of interest.

Acknowledgment

The authors would like to thank Dave Piston from the Department of Molecular Physiology and Biophysics at Vanderbilt University for the use of his microscope.

References

[1] A. Vogel and V. Venugopalan, "Mechanisms of pulsed laser ablation of biological tissues," *Chem Rev*, vol. 103, pp. 577-644., 2003.

[2] F. Hillenkamp, "Lasers in Biology and Medicine," in *Lasers in Biology and Medicine*, F. Hillenkamp, R. Pratesi, and C. A. Sacchi, Eds., ed New York: Plenum Press, 1980, p. 37.

[3] J. M. Auerhammer, R. Walker, A. F. G. van der Meer, and B. Jean, "Dynamic behavior of photoablation products of corneal tissue in the mid-IR: a study with FELIX," *Applied Physics B-Lasers and Optics*, vol. 68, pp. 111-119, Jan 1999.

[4] G. Edwards, R. Logan, M. Copeland, L. Reinisch, J. Davidson, B. Johnson, R. Maciunas, M. Mendenhall, R. Ossoff, J. Tribble, J. Werkhaven, and D. Oday, "Tissue Ablation By a Free-Electron Laser Tuned to the Amide-II Band," *Nature*, vol. 371, pp. 416-419, 1994.

[5] G. S. Edwards, R. D. Pearlstein, M. L. Copeland, M. S. Hutson, K. Latone, A. Spiro, and G. Pasmanik, "6450 nm wavelength tissue ablation using a nanosecond laser based on difference frequency mixing and stimulated Raman scattering," *Optics Letters*, vol. 32, pp. 1426-1428, Jun 1 2007.

[6] D. L. Ellis, N. K. Weisberg, J. S. Chen, G. P. Stricklin, and L. Reinisch, "Free electron laser wavelengh specificity for cutaneous contraction," *Lasers in Surgery and Medicine*, vol. 25, pp. 1-7, 1999.

[7] M. A. Mackanos, J. A. Kozub, D. L. Hachey, K. A. Joos, D. L. Ellis, and E. D. Jansen, "The effect of free-electron laser pulse structure on mid-infrared soft-tissue ablation: biological effects," *Physics in Medicine and Biology*, vol. 50, pp. 1885-1899, April 21, 2005 2005.

[8] M. A. Mackanos, J. A. Kozub, and E. D. Jansen, "The effect of free electron laser pulse structure on mid-infrared soft-tissue ablation: ablation metrics," *Physics in Medicine and Biology*, vol. 50, pp. 1871-1883, April 21, 2005 2005.

[9] M. A. Mackanos, D. Simanovskii, K. M. Joos, H. A. Schwettman, and E. D. Jansen, "Mid infrared optical parametric oscillator (OPO) as a viable alternative to tissue ablation with the free electron laser (FEL)," *Lasers in Surgery and Medicine*, vol. 39, pp. 230-236, Mar 2007.

[10] K. Nahen and A. Vogel, "Plume dynamics and shielding by the ablation plume during Er : YAG laser ablation," *Journal of Biomedical Optics*, vol. 7, pp. 165-178, Apr 2002.

[11] V. Venugopalan, N. S. Nishioka, and B. B. Mikic, "Thermodynamic response of soft biological tissues to pulsed infrared-laser irradiation," *Biophysical Journal*, vol. 71, pp. 3530-3530, Dec 1996 1996.

[12] X. G. Wang, N. T. Ishizaki, and K. Matsumoto, "Healing process of skin after CO2 laser ablation at low irradiance: A comparison of continuous-wave and pulsed mode," *Photomedicine and Laser Surgery*, vol. 23, pp. 20-26, Feb 2005.

[13] Y. Xiao, M. Guo, P. Zhang, G. Shanmugam, P. L. Polavarapu, and M. S. Hutson, "Wavelength-dependent conformational changes in collagen after mid-infrared laser ablation of cornea," *Biophysical Journal*, vol. 94, pp. 1359-1366, 2008.

[14] J. I. Youn, P. Sweet, G. M. Peavy, and V. Venugopalan, "Mid-IR laser ablation of articular and fibiro-cartilage: A wavelength dependence study of thermal injury and crater morphology," *Lasers in Surgery and Medicine*, vol. 38, pp. 218-228, 2006.

[15] T. Bende, R. Walker, and B. Jean, "Thermal Collateral Damage in Porcine Corneas after Photoablation with Free-Electron Laser," *Journal of Refractive Surgery*, vol. 11, pp. 129-136, Mar-Apr 1995.

[16] W. C. Fowler, J. G. Rose, D. H. Chang, and A. D. Proia, "The free electron laser: a system capable of determining the gold standard in laser vision correction," *Nuclear Instruments & Methods in Physics Research Section A -- Accelerators Spectrometers Detectors and Associated Equipment*, vol. 429, pp. 497-501, 1999.

[17] M. Heya, Y. Fukami, and K. Awazu, "Development of a micropulse-picking system with acousto-optic modulators for MIR-FEL/tissue interaction experiments," *Japanese Journal of Applied Physics Part 1-Regular Papers Short Notes & Review Papers*, vol. 41, pp. 143-147, Feb 2002.

[18] B. Jean and T. Bende, "Photoablation of Gelatin with the Free-Electron Laser between 2.7 Mu-M and 6.7 Mu-M," *Journal of Refractive and Corneal Surgery*, vol. 10, pp. 433-438, Jul-Aug 1994.

[19] B. Jean and T. Bende, "Infrared photoablation of the cornea," *Klinische Monatsblatter Fur Augenheilkunde*, vol. 214, pp. 195-202, 1999.

[20] J. I. Youn, G. M. Peavy, and V. Venugopalan, "Free electron laser ablation of articular and fibro-cartilage at 2.79, 2.9, 6.1, and 6.45 mu m: Mass removal studies," *Lasers in Surgery and Medicine*, vol. 36, pp. 202-209, 2005.

[21] J. I. Youn, G. M. Peavy, and V. Venugopalan, "A comparison of mass removal and crater morphology produced in cortical bone by ablation using selected mid-infrared wavelengths of a free electron laser," *Lasers in Surgery and Medicine*, p. 39, 2006.

[22] G. Edwards, M. S. Hutson, S. Hauger, J. Kozub, J. Shen, C. Shieh, K. Topadze, and K. Joos, "Comparison of OPA and Mark-III FEL for Tissue Ablation at 6.45 Microns," *SPIE, Commercial and Biomedical Application of Ultrafast and Free-Electron Lasers*, vol. 4633, pp. 194-201, 2002.

[23] G. S. Edwards, R. H. Austin, F. E. Carroll, M. L. Copeland, M. E. Couprie, W. E. Gabella, R. F. Haglund, B. A. Hooper, M. S. Hutson, E. D. Jansen, and e. al., "Free electron laser based biophyscal and biomedical instrumentation," *Review of Scientific Instrumentation*, vol. 74, pp. 3207-3245, 2003.

[24] E. D. Jansen, M. L. Copeland, G. Edwards, W. E. Gabella, K. M. Joos, M. A. Mackanos, J. H. Shen, and S. R. Uhlhorn, "Applications: Case Studies: Medical: Therapeutic Applications: Free-Electron Laser," in *Handbook of Laser Technology and Applications*. vol. 3: Applications, C. E. Webb and J. D. C. Jones, Eds., ed U.K.: Institute of Physics Publishing, 2003.

[25] K. M. Joos, L. Mawn, J. H. Shen, E. D. Jansen, and V. A. Casagrande, "Acute optic nerve sheath fenestration in humans using the free electron laser

(FEL): a case report," *in: Ophthalmic Technologies XII, F. Manns, P. Soderberg and A. Ho (eds), SPIE, Bellingham, WA*, vol. 4611, pp. 81-85, 2002.

[26] K. M. Joos, J. H. Shen, D. J. Shetlar, and V. A. Casagrande, "Optic nerve sheath fenestration with a novel wavelength produced by the free electron laser (FEL)," *Lasers Surg Med*, vol. 27, pp. 191-205, 2000.

[27] L. Reinisch, M. Mendenhall, S. Charous, and R. H. Ossoff, "Computer-assisted surgical techniques using the Vanderbilt Free Electron Laser," *Laryngoscope*, vol. 104, pp. 1323-1329, 1994.

[28] P. Bodis, R. Timmer, S. Yeremenko, W. J. Buma, J. S. Hannam, D. A. Leigh, and S. Woutersen, "Heterovibrational interactions, cooperative hydrogen bonding, and vibrational energy relaxation pathways in a rotaxane," *Journal of Physical Chemistry C*, vol. 111, pp. 6798-6804, May 10 2007.

[29] S. V. Chekalin, V. O. Kompanets, V. B. Laptev, S. V. Pigul'sky, A. A. Makarov, and E. A. Ryabov, "Intramolecular vibrational dynamics in bis(trifluoromethyl)keten excited by resonant femtosecond IR radiation," *Chemical Physics Letters*, vol. 512, pp. 178-183, Aug 25 2011.

[30] G. Hanna and E. Geva, "Isotope Effects on the Vibrational Relaxation and Multidimensional Infrared Spectra of the Hydrogen Stretch in a Hydrogen-Bonded Complex Dissolved in a Polar Liquid," *Journal of Physical Chemistry B*, vol. 112, pp. 15793-15800, Dec 11 2008.

[31] S. Twagirayezu, X. Wang, D. S. Perry, J. L. Neil, M. T. Muckle, B. H. Pate, and L.-H. Xu, "IR and FTMW-IR Spectroscopy and Vibrational Relaxation Pathways in the CH Stretch Region of CH(3)OH and CH(3)OD," *Journal of Physical Chemistry A*, vol. 115, pp. 9748-9763, Sep 1 2011.

[32] S. Amini-Nik, D. Kraemer, M. L. Cowan, K. Gunaratne, P. Nadesan, B. A. Alman, and R. J. Miller, "Ultrafast mid-IR laser scalpel: protein signals of the fundamental limits to minimally invasive surgery," *PLoS One*, vol. 5, 2010.

[33] K. Franjic, M. L. Cowan, D. Kraemer, and R. J. D. Miller, "Laser selective cutting of biological tissues by impulsive heat deposition through ultrafast vibrational excitations," *Optics Express*, vol. 17, pp. 22937-22959, Dec 7 2009.

[34] K. L. Vodopyanov, F. Ganikhanov, J. P. Maffetone, I. Zwieback, and W. Ruderman, "ZnGeP2 optical parametric oscillator with 3.8-12.4-mu m tunability," *Optics Letters*, vol. 25, pp. 841-843, Jun 1 2000.

[35] G. C. Catella, R. C. Eckardt, R. K. Shori, T. T. Stenger, and R. W. Dew, "IR laser/OPO systems for biomedical and chemical sensing," *IEEE, LEOS*, vol. 2, pp. 504-505, 2002.

[36] R. K. Shori, O. M. Satsudd, N. S. Prasad, and G. Catella, "High Energy $AgGaSe_2$ Optical Parametric Oscillator Operating in 5.7 -7 μm Region," *IEEE*, pp. 179-181, 2000.

[37] J. Kozub, B. Ivanov, A. Jayasinghe, R. Prasad, J. Shen, M. Klosner, D. Heller, M. Mendenhall, D. W. Piston, K. Joos, and M. S. Hutson, "Raman-shifted alexandrite laser for soft tissue ablation in the 6- to 7-microm wavelength range," *Biomed Opt Express*, vol. 2, pp. 1275-81, 2011.

[38] C. L. Canedy, W. W. Bewley, J. R. Lindle, J. A. Nolde, D. C. Larrabee, C. S. Kim, M. Kim, I. Vurgaftman, and J. R. Meyer, "Interband Cascade Lasers with Wavelengths Spanning 2.9 mu m to 5.2 mu m," *Journal of Electronic Materials*, vol. 37, pp. 1780-1785, Dec 2008.

[39] J. Faist, F. Capasso, D. L. Sivco, C. Sirtori, A. L. Hutchinson, and A. Y. Cho, "QUANTUM CASCADE LASER," *Science*, vol. 264, pp. 553-556, Apr 22 1994.

[40] P. Q. Liu, A. J. Hoffman, M. D. Escarra, K. J. Franz, J. B. Khurgin, Y. Dikmelik, X. Wang, J.-Y. Fan, and C. F. Gmachl, "Highly power-efficient quantum cascade lasers," *Nature Photonics*, vol. 4, pp. 95-98, Feb 2010.

[41] K. Becker, J. B. Johnson, and G. Edwards, "Broad-Band Pockels Cell and Driver for a Mark III-Type Free-Electron Laser," *Review of Scientific Instruments*, vol. 65, pp. 1496-1501, May 1994.

[42] D. C. Lamb, J. Tribble, A. G. Doukas, T. J. Flotte, R. H. Ossoff, and L. Reinisch, "Custom designed acoustic pulses," *Journal of Biomedical Optics*, vol. 4, pp. 217-223, 1999.

[43] C. A. Brau, *Free Electron Lasers*. Boston: Academic Press, 1990.

[44] G. Edwards, D. Evertson, W. Gabella, R. G. R, T. King, J. Kozub, M. Mendenhall, J. Shen, R. Shores, S. Storms, and R. Traeger, "Free-Electron Lasers: Performance, Reliability, and Beam Delivery," *IEEE Journal of Special Topics in Quantum Electronics*, vol. 2, 1996.

[45] G. S. Edwards and M. S. Hutson, "Advantage of the Mark-III FEL for biophysical research and biomedical applications," *Journal of Synchrotron Radiation*, vol. 10, pp. 354-357, Sep 2003.

[46] J. M. Khosrofian and B. A. Garetz, "Measurement of a Gaussian Laser-Beam Diameter through the Direct Inversion of Knife-Edge Data," *Applied Optics*, vol. 22, pp. 3406-3410, 1983.

[47] M. S. Hutson, S. A. Hauger, and G. Edwards, "Thermal diffusion and chemical kinetics in laminar biomaterial due to heating by a free-electron laser," *Physical Review E*, vol. 65, pp. Art. No.-061906, 2002.

[48] J. T. Walsh and T. F. Deutsch, "Pulsed CO2-Laser Ablation of Tissue - Effect of Mechanical-Properties," *IEEE Transactions On Biomedical Engineering*, vol. 36, pp. 1195-1201, 1989.

[49] J. R. Vazquez de Aldana, C. Mendez, and L. Roso, "Saturation of ablation channels micro-machined in fused silica with many femtosecond laser pulses," *Optics Express*, vol. 14, pp. 1329-1338, Feb 6 2006.

[50] B. Majaron and M. Lukac, "Calculation of crater shape in pulsed laser ablation of hard tissues," *Lasers in Surgery and Medicine*, vol. 24, pp. 55-60, 1999 1999.

[51] O. V. Borisov, X. L. Mao, and R. E. Russo, "Effects of crater development on fractionation and signal intensity during laser ablation inductively coupled plasma mass spectrometry," *Spectrochimica Acta Part B-Atomic Spectroscopy*, vol. 55, pp. 1693-1704, Nov 1 2000.

[52] A. D. Zweig, "A Thermomechanical Model For Laser Ablation," *Journal of Applied Physics*, vol. 70, pp. 1684-1691, Aug 1 1991.

[53] E. D. Jansen, T.-G. van-Leeuwen, and M. Motamedi, "Partial vaporization model for pulsed mid-infrared laser ablation of water," *Journal of Applied Physics*, vol. 78, pp. 564-571, 1995.

[54] S. R. Uhlhorn, "Free electron laser ablation of soft tissue: The effects of chromophore and pulse characteristics on ablation mechanics," *Ph.D. Thesis, Vanderbilt University*, 2002.

[55] M. Ith, M. Frenz, and H. P. Weber, "Scattering and thermal lensing of 2.12-mu m laser radiation in biological tissue," *Applied Optics*, vol. 40, pp. 2216-2223, 2001.

[56] M. Motamedi, A. J. Welch, W. F. Cheong, S. A. Ghaffari, and O. T. Tan, "Thermal Lensing in Biologic Medium," *Ieee Journal of Quantum Electronics*, vol. 24, pp. 693-696, 1988.

[57] R. L. Vincelette, A. J. Welch, R. J. Thomas, B. A. Rockwell, and D. J. Lund, "Thermal lensing in ocular media exposed to continuous-wave near-infrared radiation: the 1150-1350-nm region," *Journal of Biomedical Optics*, vol. 13, 2008.

Mark Mackanos received his B.S., M.S., and Ph.D. degrees in Biomedical Engineering from Vanderbilt University, Nashville, TN, USA in 1998, 2001, and 2004 respectively.

He was a Research Associate in the Vanderbilt University, Department of Biomedical Engineering performing soft-tissue ablation studies with a free electron laser and a ZGP:OPO in 2005. From 2005 to 2009 he was a Postdoctoral Fellow in the Stanford University, Department of Pediatrics, Stanford, CA and the Department of Veterans Affairs, Palo Alto Health Care System, Palo Alto, CA performing studies on the effects of laser energy on the healing of bone and soft-tissue and the survivability of cells related to heat shock promoters (HSP's) and other markers**,** examined up-regulation of genes responsible for cell protection and survival in tissues after laser heating with microarray and PCR analysis**,** compared heating responses to tissue between focused ultrasound and laser energy on an Hsp70 bioluminescent reporter mouse, development of an *in vivo* endoscopic fiber probe for cancer detection in the colon, esophagus, and prostate using FTIR**,** soft-tissue ablation studies with a $ZnGeP_2$ optical parametric oscillator (ZGP:OPO) and other mid-IR lasers, performed thermal targeting and release of drugs from nanoparticles, and compared Hsp70 bioluminescence to live/dead assay following laser thermal stress on the retina for diabetic retinopathy. He is currently a Research Assistant Professor in the Vanderbilt University, Department of Biomedical Engineering performing research on laser, thermal, and biological studies of the mechanism for optical nerve stimulation; confocal microscopy, optical coherence tomography, and Raman spectroscopy analysis on human skin for the detection of cancers; and soft-tissue ablation studies with a tunable mid-IR compressed hydrogen Raman laser. He is the author or co-author of more than twenty scholarly articles and book chapters.

He is currently a member of The International Society for Optics and Photonics (SPIE).

Dmitrii Simanovskii received the M.S. degree in physics from Leningrad, Politechnical Institute, Leningrad, Russia in 1984 and the Ph.D. degree in physics from the A.F. Ioffe Physico-Technical Institute, Leningrad, Russia in 1988.

He was a Research Scientist at the A.F. Ioffe Physico-Technical Institute performing research on x-ray generation in laser produced plasmas and x-ray diagnostics of high temperature plasmas from 1988 to 1996. He was a Visiting Scientist at the Institute for Quantum Optics, Hannover University, Hannover, Germany performing research on coherent x-ray generation and diagnostics in laser-produced plasmas from 1997 to 1998. He was a Research Associate at the Hansen Experimental Physics Lab, Stanford University, Stanford, CA performing mid-IR ablation of organic and inorganic materials and tissues, CARS microscopy design, plasma mediated ablation of bone, scanning near-field infrared spectroscopy, and the design of an optical system for optoelectronic retinal prosthesis from 1999 to 2003. He was a Senior Research Scientist in the Hansen Experimental Physics Lab, Stanford University from 2003 to 2008. He is currently a Research Scientist at Coherent, Inc., Mountain View, CA.

Kenneth Schriver received the B.A. degree in Chemistry from Reed College, Portland, OR, USA in 1985 and the Ph.D. in Physical Chemistry from the University of California Los Angeles, Los Angeles, CA, USA in 1990.

He was a Technical Manager, Vice President, and Senior Vice President of Lion Industries Inc., Vancouver, WA, USA from 1989 to 1991, 1991 to 1994, and 1994 to 1996 respectively. He was the Director of Technology at Vinings Industries Inc., Kennesaw, GA, USA from 1996 to 2001. He was a Research Assistant Professor of Physics , Vanderbilt University, Nashville, TN, USA from 2001 to 2005, a Senior Lecturer of Physics, Vanderbilt University from 2005-2010. He is currently a Research Assistant Professor of Physics at Vanderbilt University. His current research involves infrared matrix-assisted laser desorption/ionization (IR-MALDI), high spatial resolution MALDI imaging mass spectrometry, and resonant infrared pulsed-laser deposition (RIR-PLD).

Dr. Schriver is a member of the American Association for the Advancement of Science (AAAS), the American Association of Physics Teachers (AAPT), the American Chemical Society (ACS), the American Physical Society (APS), the American Society for Mass Spectrometry (ASMS), and the International Society for Optics and Photonics (SPIE).

M. Shane Hutson received his B.A and M.S. degrees in physics from Wake Forest University, Winston-Salem, NC in 1992 and 1993 and received a Ph.D. in biophysics from the University of Virginia, Charlottesville, VA in 2000. He was a Postdoctoral Fellow at the Duke University Free Electron Laser Laboratory from 2000-2003. He joined the faculty of the Department of Physics at Vanderbilt University in 2003.

He is currently an Associate Professor of Physics at Vanderbilt University with a courtesy appointment in the Department of Biological Sciences. His research interests include experimental and computational approaches to understanding the mechanisms of soft tissue ablation with mid-IR lasers, as well as the use of laser microsurgery as an *in vivo* tool to investigate the cellular mechanics of embryogenesis.

Dr. Hutson is a member of the American Physical Society and the Biophysical Society.

Christopher Contag received his B.S. degree in Biology and his Ph.D. in Microbiology from the University of Minnesota, Minneapolis, MN, USA in 1982 and 1988 respectively.

He was a Postdoctoral Fellow in the Department of Pediatrics, Stanford University School of Medicine, Stanford, CA from 1989-1995. He was an Assistant Professor in the Departments of Pediatrics and Microbiology and Immunology at the Stanford University School of Medicine, Stanford, CA from 1997-2005 with a courtesy appointment in the Department of Radiology from 1998-2004. He was the director of the Medical Free Electron Laser Program, Stanford University, now called the Stanford Program in Military Photomedicine. He is currently the Director of the Stanford Center for Innovation in In Vivo Imaging, Director of the Stanford Program in Military Photomedicine, the Co-director of the Molecular Imaging Program at Stanford, a Member of the Administrative Committee at the Hansen Experimental Physics Laboratory at Stanford University, an Associate Professor in the Departments of Pediatrics, Microbiology & Immunology and, by courtesy, of the Department of Radiology at Stanford University School of Medicine, Stanford CA.

Dr. Contag was the President of the Society for Molecular Imaging in 2002. He was the Founder of Xenogen Corporation, Alameda, CA 1995 and served as its president from 1995 to 1997. He Founded ConcentRx Corporation in 2007. He is currently a member of the editorial boards for Molecular Imaging, Cancer Biology and Therapy, and Disease Models and Mechanisms.

John Kozub received the B.S. degree in physics from Tennessee Technological University, Cookeville, TN, USA in 1987, and the Ph.D. degree in physics from Vanderbilt University, Nashville, TN, USA, in 1995. His postdoctoral work at Vanderbilt involved research into the interaction of proteins and DNA with UV and mid-IR pulsed laser light. In 1997, he joined the Vanderbilt W.M. Keck Free Electron Laser Center as a research engineer, where he was closely involved with ongoing research into accelerator physics, condensed matter optics, and medical applications of pulsed lasers. His work at the FEL Center focused on laser beam diagnostics and involved the maintenance and optimization of a free electron laser, a variety of solid state lasers, ultrafast lasers, and optical parametric generators.

In 2005, he became Associate Director of the Free Electron Laser Center, a position he held until the center closed in 2008. He is currently a research engineer at Vanderbilt University involved in several different research projects using ultrafast lasers to investigate optical properties of condensed matter and using a Raman-shifted Alexandrite laser to investigate surgical applications of mid-IR pulsed lasers. His research interests include laser tissue ablation, infrared spectroscopy of biological molecules, and non-linear optics.

E. Duco Jansen received his M.S. (Drs) degree in Medical Biology from the University of Utrecht, Utrecht, The Netherlands in 1990, and the M.S. and Ph.D. degrees in Biomedical Engineering from the University of Texas at Austin in 1992 and 1994 respectively.

He is currently a Professor of Biomedical Engineering and Neurosurgery at Vanderbilt University and is the Director of Graduate Studies of the Biomedical Engineering Department at Vanderbilt University. Dr. Jansen His research interests include novel approaches to optically probe and manipulate the neural system, mechanisms of pulsed laser ablation of biological tissue, cellular and biochemical responses of biological tissue to laser radiation, medical applications of lasers. He has published nearly 100 scholarly articles and book chapters in addition to approximately 250 conference abstracts and proceedings.

Dr. Jansen is a Fellow of the SPIE (The International Society for Optics and Photonics), AIMBE (American Institute for Medical and Biological Engineering) and ASLMS (American Society for Laser Surgery and Medicine). He served as President of the latter in 2010/11.